Increases in Guinea Pig Small Intestinal Transepithelial Resistance Induced by Osmotic Loads Are Accompanied by Rapid Alterations in Absorptive-Cell Tight-Junction Structure

JAMES L. MADARA
Department of Pathology, Harvard Medical School and Brigham and Women's Hospital, Boston, Massachusetts 02115

ABSTRACT In some epithelia, mucosal exposure to osmotic loads produces an increase in transepithelial resistance that is presumed to relate to the collapse of the paracellular spaces. Since proximal small intestinal epithelium may transiently encounter osmotic loads during normal digestion, we examined the short-term effect of osmotic loads on resistance and on epithelial structure of mucosal sheets prepared from guinea pig jejunum using Ussing-chamber, thin-section electron-microscopic, and freeze-fracture techniques. After equilibration of mucosal sheets in chambers, mucosal buffer tonicity was increased to 600 mosM with mannitol. This resulted in a 64% increase in resistance within 20 min. Concomitantly, 600 mosM produced a decrease in tight-junction cation selectivity as judged from dilution potentials, collapse of paracellular spaces, decreased cytoplasmic electron density in 10–40% of absorptive cells, and focal absorptive-cell subjunctional lateral-membrane evaginations often associated with microfilament arrays. Freeze-fracture replicas of absorptive-cell tight junctions revealed significant increases in both strand count and depth. Preincubation with 5 μg/ml cytochalasin D reduced the 600 mosM resistance increase caused by 600 mosM exposure by 48% but did not prevent the collapse of paracellular spaces. Lowered temperatures that produced morphologic evidence consistent with a gel-phase transition of absorptive-cell lateral membranes prevented both the resistance response and the alterations in tight-junction structure. In conclusion, transient osmotic loads produce an increase in resistance in jejunal epithelium and alter both absorptive-cell tight-junction charge selectivity and structure. These responses, which may have physiologic implications, can be reduced by cytoskeletal inhibitors and ablated by conditions that restrict mobility of absorptive-cell lateral-membrane molecules.

Brief (20-min) exposure of the mucosal surface to hyperosmotic loads may elicit an increase in electrical resistance to passive transepithelial ionic flow in some low-resistance epithelia (1, 2). Since the vast majority of passive ion flow in low-resistance epithelia occurs through the paracellular pathway (3), it is presumed that these transepithelial resistance increments are caused by increased paracellular resistance to ion flow (1). Moreover, based on morphological observations, it has been suggested that this resistance increase may be due to collapse of the epithelial intercellular spaces (1). Indeed the partial obliterations of intercellular spaces following exposure to osmotic loads is the major evidence cited to support the notion that the width of the intercellular space influences transepithelial resistance (3, 4). Since the mucosal surface of the proximal small intestine, which is lined by a low-resistance epithelium, experiences transient mucosal osmotic loads during the process of normal digestion, we studied in vitro the effects of brief mucosal hyperosmotic loads on transepithelial electrical resistance and epithelial structure in guinea pig jejunum. Furthermore, since (*a*) tight junctions appear to contribute to the regulation of paracellular molecular flow (5–10), (*b*) tight-junction structure often correlates with transepithelial resistance (6, 11, 12), and (*c*) tight junction structure can, under some conditions, be dramatically altered within minutes (13, 14), we analyzed structural features of absorptive-cell tight junctions in replicas of freeze-fractured mucosa both before and after exposure to mucosal hyperosmotic loads. Since the cytoskeleton may influence tight-junction

THE JOURNAL OF CELL BIOLOGY · VOLUME 97 JULY 1983 125-136

structure (15) and since alterations in the structure of the tight junction would presumably require movement of junctional subunits within the plane of the lateral membrane, we also studied the effects of chemical agents that interfere with cytoskeletal function and of alterations in temperature that influence molecular motion in the plasma membrane on the osmotically induced alteration of jejunal transepithelial resistance. We also used dilution potentials to assess alterations in tight-junction charge selectivity under conditions of mucosal osmotic loads.

MATERIALS AND METHODS

For these experiments, 12–15-cm segments of proximal jejunum starting at the ligament of Treitz were obtained from 78 Hartley-strain guinea pigs (Elm Hill Farms, Chelmsford, MA) weighing 400–600 g. All animals were fasted overnight before use and were anesthetized with Nembutal. Unless otherwise stated, all functional and structural observations were based on tissues from at least four experiments.

Physiological Techniques: Jejunum was rapidly removed, opened, washed in chilled oxygenated buffer, and cut into 2-cm segments. After the serosa and external longitudinal layer of the muscularis propria were stripped away, these subsegments were mounted in Ussing chambers equipped with two calomel voltage sensitive electrodes and two Ag-AgCl curent passing electrodes. Electrodes were connected to the chamber solution via agar bridges. Both mucosal (M) and serosal (S) sides of the chamber were attached to circulating 10-ml reservoirs driven by a gas lift column of 95% O_2-5% CO_2. The reservoirs were jacketed with a circulating water-bath, which was maintained at 37°C unless otherwise specified. After a 15-min equilibration period, base-line resistance was determined. Base-line tissue resistance was recorded as the absolute resistance reading minus the fluid resistance. Since 600-mosM solutions raised the fluid resistance of the entire chamber by a mean of 3.96 $\Omega \cdot cm^2$, half of this value (2 $\Omega \cdot cm^2$) was subtracted (along with isotonic fluid resistance) from resistance values recorded under conditions in which half the chamber (mucosal side) contained 600-mosM solutions. The initial equilibration was carried out with buffer solution consisting of (in millimolar): 114, NaCl; 5, KCl; 1.65, Na_2PO_4; 0.3, NaH_2PO_4; 25, $NaHCO_3$; 1.25, $CaSO_4$; and 1.1, $MgSO_4$ at pH 7.4. 20 mM glucose was added to the S buffer and 20 mM mannitol was added to the M buffer. Hyperosmolar solutions were prepared by adjusting the osmolarity of the buffer solution with mannitol.

Morphologic Techniques: Jejunal mucosal sheets from all experiments were examined by 1-μm toluidene blue-stained sections. In addition, as indicated below, representative mucosal samples from various experimental conditions were examined by freeze-fracture and/or electron microscopy of thin sections.

At the end of all experiments, tissues were fixed in the chambers by gradually adding 1 ml of 25% glutaraldehyde to both M and S reservoirs, resulting in a final glutaraldehyde concentration of 2.5%. After 20 min, the tissues were removed from the chambers and fixed for an additional 2 h at 4°C in a solution of 2% formaldehyde, 2.5% glutaraldehyde, and 0.4% $CaCl_2$ in 0.1 M sodium cacodylate buffer (16). Tissues for freeze-fracture were embedded in 3% agar and cut into 150-μm slices with a Smith-Farquhar tissue chopper. After equilibrating for 1 h in 20% glycerol in 0.1 M sodium cacodylate buffer, tissue slices were mounted between two gold discs, rapidly frozen in partially solidified Freon 22, and stored in liquid nitrogen. Specimens were fractured at a stage temperature of −110°C in a Balzers 300 freeze-etch device, replicated with platinum-carbon, cleaned in commercial bleach, and mounted on formvar-coated 200-mesh hexagonal grids.

For quantitative evaluation of absorptive-cell tight-junction structure, 21 replicas of mucosal sheets from four control animals and 24 replicas of mucosal sheets from four experimental animals were examined. Control replicas were obtained from mucosal sheets that had been mounted in Ussing chambers and perfused with isotonic buffer for a period of time equivalent to the total time the experimental sheets were in chambers. All replicated absorptive-cell tight junctions encountered that measured at least 1 μm in width were photographed at a screen magnification of × 15,000. The negatives were mounted on an illuminated viewing box, and tight-junction structure was analyzed with a 10× ocular micrometer. Average depth was determined by measuring the distance between the uppermost and lowermost strands at a point one-fourth the distance from the ends of each exposed tight junction. At the same points, P-face strands and E-face furrows intersecting the vertically placed micrometer bar were counted. A total of 168 experimental and 210 control junctions were analyzed. Additionally, 75 absorptive cell tight junctions were similarly examined in tissues exposed to cytochalasin D and subsequently to 600 mosM mucosal buffer.

After initial aldehyde fixation, tissues for conventional electron microscopy of thin sections were washed in 0.1 M sodium cacodylate, postfixed for 1 h in 1% osmium tetroxide, dehydrated in a graded series of alcohols, and embedded in epoxy resin. Oriented villi were selected from toluidene blue-stained 1-μm sections. Representative thin sections were mounted on copper-mesh grids and stained with uranyl acetate and lead citrate.

Replicas and thin sections were examined and photographed in a Philips 201 electron microscope.

Hyperosmotic Loads: To determine the time sequence and polarity of the effect of osmotic loads, we exposed mucosal sheets to the following conditions for 60 min following the 15-min equilibration period: (*a*) isotonic buffer M and S; (*b*) 600 mosM buffer M, isotonic buffer S; (*c*) isotonic buffer M, 600 mosM buffer S; and (*d*) 600 mosM buffer M and S. To assess the morphological effects of brief periods of mucosal osmotic loads, we fixed other mucosal sheets 10 or 20 min after exposure to either M 600 mosM or isotonic buffer. The effects on resistance and epithelial structure of 450 mosM M for 20 min were assessed and compared with the effects of 600 mosM M on sheets prepared from adjacent tissue. The physiological and structural effects of reversal to isotonic M after exposure to 600 mosM M for 10 or 20 min were also assessed.

Effects of Chemical and Physical Agents on Osmotically Induced Changes in Resistance: For these experiments the effect of various chemical and physical agents on transepithelial resistance responses induced by 20-min exposure to 600 mosM M, isotonic S was assessed.

To assess the effects of inhibitors of cytoskeletal function, we added cytochalasin B or D (Sigma Chemical Co., St. Louis, MO) to the isotonic mucosal solution during the 15-min equilibration period at a dose of 5 μg/ml. When the mucosal solution was replaced with 600 mosM hyperosmotic solution, the same dose of cytochalasin was again added. In addition, the effects of mucosal exposure to two plant-derived cytokinins, zeatin (1.25 mM) and kinetin (0.4 mM) (Sigma Chemical Co.), which are known to affect transepithelial resistance in *Necturus* gallbladder (15), were similarly studied. The above agents were solubilized in dimethyl sulfoxide (DMSO), and the final DMSO concentration in the mucosal bath was always <1%, a concentration which, in separate experiments, showed no effect on transepithelial resistance. The effect of colcemid on the osmotically-induced resistance response was studied in three animals. Colcemid was injected 0.5 mg/kg i.p. 1.5 h before sacrifice. Jejunal mucosal sheets were then exposed to 600 mosM mucosal solutions for 20 min after the standard equilibration period and the increment in resistance was compared with that of similarly exposed mucosal sheets from control animals. The effects of preequilibration with mucosal and serosal cycloheximide, at a dose (0.5 mg/ml) that is known to inhibit >90% of intestinal epithelial cell protein synthesis (17), on the resistance response to osmotic loading was studied. Lastly, the effects on transepithelial resistance of 600 mosM M loads were studied at 4°C, a temperature below the phase transition temperature of absorptive-cell basolateral membranes on the mammalian small intestine as determined by fluorescence polarization and differential scanning calorimetry (18).

Effects of Mucosal Osmotic Loads on Junctional Charge-Selectivity: To assess charge selectivity of the paracellular shunt pathway, we measured dilution potentials in mucosal sheets exposed to 600 mosM M and sheets exposed to M and S isotonic buffer. After 20-min exposure to 600 mosM M the mucosal solution was switched to isotonic buffer. After an additional 5 min, by which time the spontaneous electrical potential difference had stabilized, the Na^+ and Cl^- in the mucosal bath was diluted 10 or 20% by removing either 1 or 2 cm^3 of mucosal buffer and replacing it with an equal volume of water made isotonic with mannitol. 5 min later, when the potential difference had again stabilized, the transepithelial potential difference, in millivolts, was read. The result was expressed as the increment in potential difference produced by dilution.

Comparisons between control and experimental data were made using the two-tailed *t* test. Results are expressed as the means ± SEM.

RESULTS

Effects of Osmotic Loads on Transepithelial Resistance

The transepithelial resistance of mucosal sheets bathed with isotonic M and S buffer remained relatively stable for at least 75 min (Fig. 1). However, exposure to 600 mosM M resulted in a 64% increase ($P < 0.001$) in resistance, which peaked at 15–20 min and returned toward base line over the next 40 min (Fig. 1). Exposure to the same osmotic gradient but of reversed polarity (isotonic M, 600 mosM S) had no significant

effect on resistance, and exposure to 600 mosM M and S resulted in a gradual decline in resistance over 60 min (Fig. 1).

Exposure to 450 mosM M resulted in a resistance increment intermediate between that of isotonic M and that of 600 mosM M (Fig. 2). Changing the mucosal solution to isotonic buffer after 20-min exposure to jejunal sheets to 600 or 450 mosM M resulted in a return in resistance toward base-line values within 20 min. In separate experiments it was found that early reversal to isotonic mucosal solutions after 10 min of 600 mosM M exposure prevented the subsequent resistance peak and resulted in a decrease in resistance toward base-line levels.

Effects of Osmotic Loads on Epithelial Structure

60-MIN EXPOSURE: 1-μm sections of toluidene blue-stained mucosal sheets exposed to isotonic buffer showed no evidence of epithelial injury. Preparations exposed to M and S 600 mosM solutions showed extensive epithelial cell damage including vacuolization, marked extrusion, and focal disruption of the villus epithelial barrier. Sheets exposed to 600 mosM on the mucosal side only showed qualitatively similar but less severe damage to villus epithelial cells. Since 60-min exposure to mucosal osmotic loads resulted in damage to the epithelium with sloughing of epithelial cells, we did not further study these tissues. Rather, as outlined below, we concentrated our studies on the 20-min period immediately following 600 mosM mucosal exposure. Exposure to 600 mosM S, isotonic M showed an intact epithelial layer but 1–5-μm vacuoles were seen in the apical cytoplasm of villus absorptive cells.

20-MIN MUCOSAL EXPOSURE: Since rapid increases in transepithelial resistance resulted from mucosal but not serosal osmotic loads, we chose to study, in detail, preparations after exposure to mucosal osmotic loads. In addition, since the resistance peak occurred in 20 min and prolonged in vitro exposure resulted in extensive epithelial damage, focal denudation, and marked cell extrusion, we chose to examine the effects of 20-min 600 mosM M exposure. Mucosal sheets so treated displayed a characteristic appearance in 1-μm sections: the epithelium remained intact; however, ~10–40% of villus absorptive cells displayed a marked decrease in the intensity of cytoplasmic staining with toluidine blue and an apparent increase in cell volume (Fig. 3*B*). These cells were randomly scattered over the upper half of the villus and were intermixed with normal-appearing villus epithelial cells. The luminal border of the epithelium also became markedly scalloped in the upper half to two-thirds of the villi. It must be emphasized that, as shown in Fig. 3*B*, only epithelial cells on the villus (absorptive cells) displayed these structural alterations. The minor population of goblet cells on the villus was not so affected.

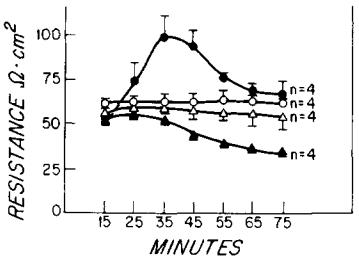

FIGURE 1 Effects of hyperosmotic exposure on transepithelial resistance of mucosal sheets prepared from guinea pig jejunum. Exposure of the mucosal surface only to 600 mosM induces a transient rise in resistance that peaks in 20 min. Exposure to serosal 600 mosM only has no significant effect. Simultaneous exposure of both surfaces to 600 mosM results in a gradual decrease in resistance. O, isotonic mucosa and serosa; ●, 600 mosM mucosa, isotonic serosa; △, 600 mosM serosa, isotonic mucosa; ▲, 600 mosM mucosa and serosa.

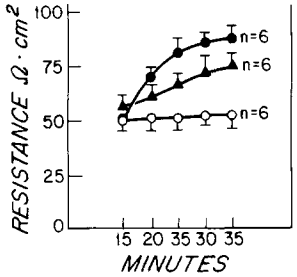

FIGURE 2 Effects of graded mucosal hyperosmotic exposure on transepithelial resistance. Mucosal exposure to 450 mosM mucosal (▲) for 20 min results in a resistance intermediate between those of control (isotonic mucosal, O) and 600 mosM (●) exposed sheets.

Electron microscopy of thin sections demonstrated that the clear cells seen in 1-μm sections represented absorptive cells with decreased cytoplasmic density, slightly convex apical surfaces, and multiple cytoplasmic vesicles measuring 0.1 μm in diameter (Fig. 4). Occasionally, these absorptive cells had subjunctional evaginations of the lateral membrane that were often associated with arrays of microfilaments and were devoid of cytoplasmic organelles (Figs. 5 and 6). The remaining absorptive cells had denser cytoplasmic staining but consistently demonstrated multiple 0.1-μm membrane-bounded vesicles within the terminal web (Fig. 5). Frequently, absorptive-cell apical membranes at sites adjacent to tight junctions lost their microvilli and became smooth and convex (Fig. 6). This finding was noted both at "clear" cell to "normal" cell and normal cell to normal cell junctions. Lastly, the paracellular spaces of tissues exposed mucosally to 600 msoM solutions showed close apposition of the lateral membranes of adjacent epithelial cells both in the crypt and on the villus. Occasionally, however, particularly in the area of interdigitations, focal dilitation of this space was noted (Fig. 4). Mucosal sheets exposed for 20 min to 450 mosM mucosal loads demonstrated qualitatively similar but much less pronounced structural changes. Structural alterations similar to those described above were not present in sheets exposed only to isotonic solutions when assessed by light (Fig. 3*A*) or electron microscopy. In addition, control sheets showed extensive variation in the width of the paracellular space. Reversal of mucosal solutions to isotonic buffer for 20 min after the period of exposure to M 600 mosM resulted in a loss of the above structural alterations. However, such tissues showed extrusion of many absorptive cells from the mucosal surface (Fig. 3*D*). Similar reversal experiments after mucosal exposure to 450 mosM solutions for 20 min also demonstrated loss of the above osmotically induced structural alterations but these sheets showed little evidence of epithelial sloughing.

Freeze-fracture analysis of absorptive-cell tight-junction structure revealed increases in both strand count (5.3 to 6.3, $P < 0.005$) and depth (266 to 303 nm, $P < 0.005$) in tissues exposed to 600 mosM vs. controls (Table I). Expressing the data as histograms (Figs. 7 and 8) we showed that these increases were not due to a uniform shift in these structural parameters. Rather, these increases were due to the introduction of a new subpopulation of tight junctions consisting of focal deep multistranded areas (Fig. 9, *B* and *C*). Many of these foci occurred at sites with sparse microvilli and apical membrane convexity (Fig. 9*C*). Thus, these regions of junctional proliferations may, in part, correspond to the parajunctional apical membrane convexities seen in thin sections. Another characteristic feature of these proliferated junctional areas was their association with sharp curves of the lateral membrane, which may correspond to the lateral membrane

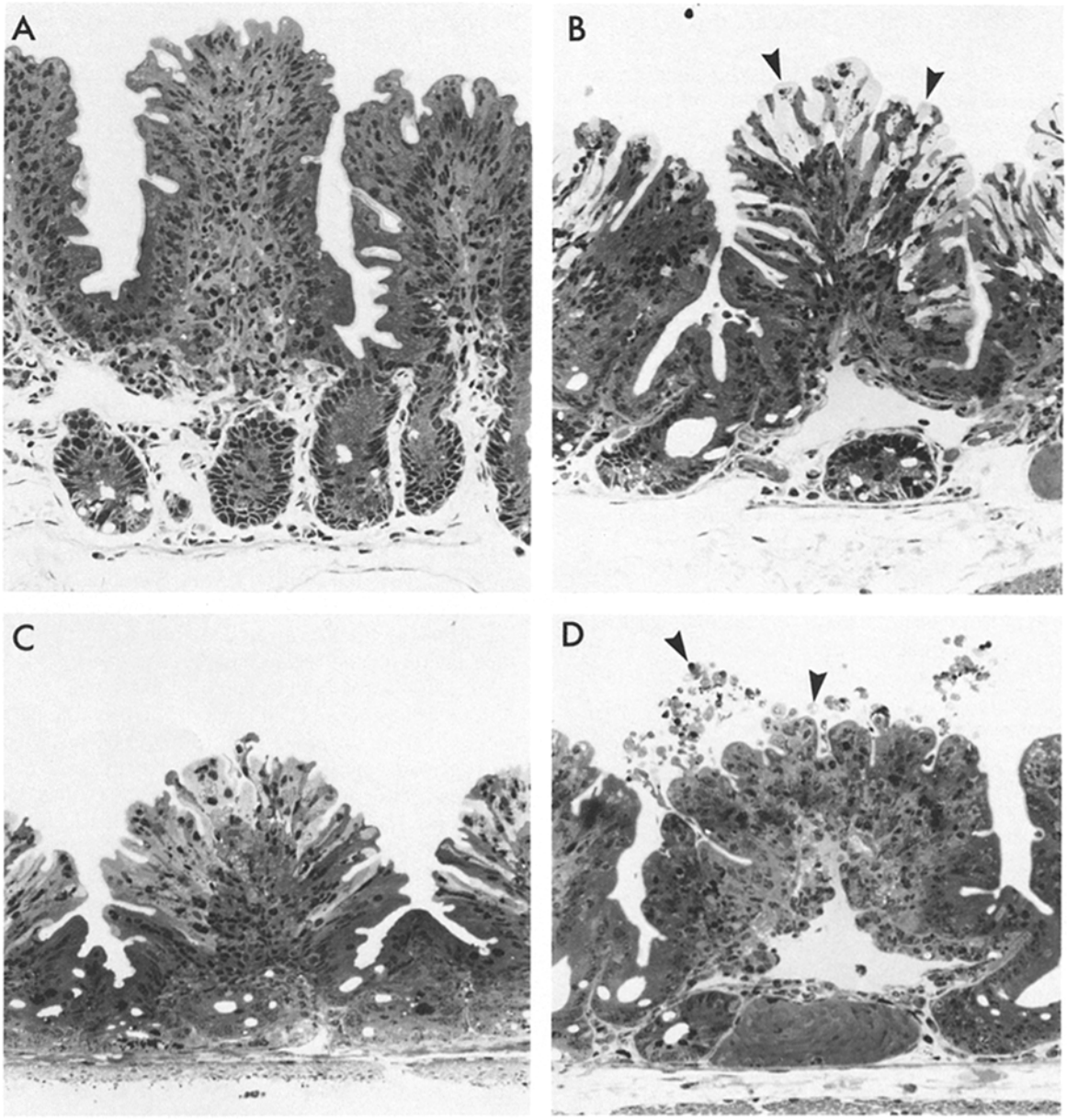

FIGURE 3 Light micrograph of jejunal mucosal sheets after exposure to in vitro manipulations. (*A*) Control sheet exposed to isotonic Ringer's for 20 min after the initial 15-min equilibration period. Normal mucosal architecture is retained. (*B*) Jejunal sheet exposed to 20-min mucosal 600 mosM buffer after initial 15-min equilibration period with isotonic Ringer's. The villus surface is scalloped and 10–40% of villus absorptive cells display marked cytoplasmic lucency (arrowheads). (*C*) Jejunal sheet treated as in *B* but exposed during the equilibration period to 5 μg/ml mucosal cytochalasin D. The morphological appearance of this epithelium is identical to that shown in *B*. (*D*) Jejunal sheet exposed as in *B* with subsequent reversal to mucosal isotonic buffer for 20 min. Absorptive cells with lucent cytoplasm are no longer apparent; however, several villus epithelial cells appear to have been extruded (arrowheads) into the lumen. All are approximately × 200.

evaginations seen in thin section (Figs. 5 and 6). Indeed a substantial number of junctional areas that could not be quantitated, for technical reasons (focal replica collapse; inappropriate shadow angle), appeared to be deep and multistranded. Such technical problems might be expected to occur with greater frequency in areas of sharp membrane curvature. Freeze-fracture replicas prepared from tissues exposed to cytochalasin D and subsequently to 600 mosM mucosal buffer for 20 min showed rare foci of tight junctions that appeared somewhat expanded in depth and strand count and were associated with minimal ballooning of the perijunctional apical membrane. However, in contrast with the more frequently encountered expanded tight junctions in epithelia exposed to 600 mosM in the absence of cytochalasin D (Figs. 7 and 8), none of the measurements of tight-junction structure in these tissues showed strand counts exceeding 9 or depths exceeding 650 nm.

Effects of Chemical and Physical Agents of Osmotically Induced Resistance Changes

Pre-incubation for 15 min with 5 μg/ml cytochalasin D in the mucosal reservoir reduced the subsequent 600 mosM induced resistance increase by 48% ($P < 0.02$) (Fig. 10). However, the light (Fig. 3*C*) and electron microscopic appearances of these mucosal sheets were not appreciably dif-

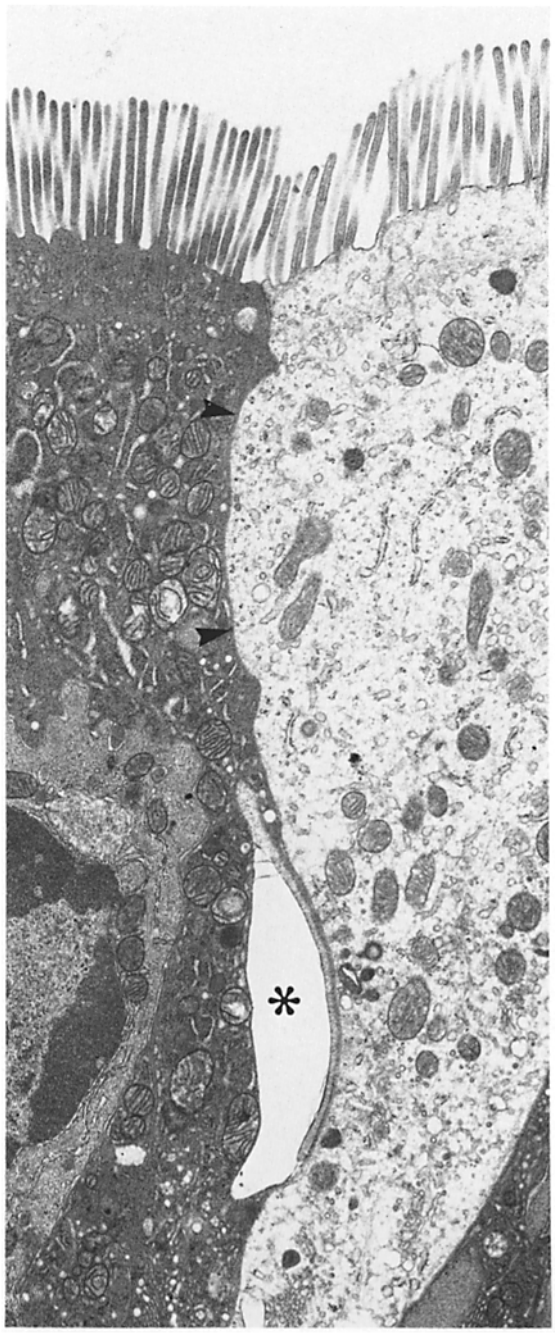

FIGURE 4 Electron micrograph of villus absorptive cells from mucosal sheet exposed for 20 min in vitro to 600 mosM mucosal buffer. The epithelial cell with the electron-lucent cytoplasm seen on the right corresponds with the clear cells seen by light microscopy. Such cells are randomly scattered among others which display a more normal appearance such as that seen on the left. The paracellular space (arrowheads) is collapsed. However, focally, particularly in areas of interdigitation, small expansions of the paracellular spaces could be noted (asterisk). × 7,400.

FIGURE 5 Electron micrograph of absorptive cells from mucosal sheets exposed to 600 mosM mucosal buffer for 20 min. The cytoplasm of lucent cells is filled with many membrane-bounded vesicles. In addition, similar vesicles are noted in the region of the terminal web of the adjacent nonlucent cell (asterisk). Subjunctional evaginations (small arrowheads) free of organelles were often found in mucosal 600 mosM exposed sheets and frequently had associated dense plaques of microfilaments (large arrowhead). × 9,200.

ferent from those of sheets not treated with cytochalasin D. Exposure of mucosal sheets bathed with isotonic buffer to cytochalasin D had no effect on transepithelial resistance (Fig. 10) or on mucosal structure as judged by light and electron microscopy.

Cytochalasin B and kinetin, at the doses used, had no effects on the base-line resistance of mucosal sheets bathed with isotonic buffer nor did they prevent the rise in resistance associated with 20-min exposure to mucosal 600 mosM. Similarly, cycloheximide at a dose that inhibits >90% of protein synthesis by small intestinal epithelial cells (17) had no effect on base-line resistance and did not ablate the 600 mosM-induced resistance rise. However, mucosal exposure to zeatin both induced a rise ($P < 0.01$) in resistance in tissues bathed with isotonic solution and reduced ($P < 0.01$) the rise in resistance associated with 600 mosM M exposure (Fig. 11).

Exposure to 600 mosM M at 4°C prevented the rise in resistance (Fig. 12). However, the base-line resistance of mucosal sheets was substantically higher than that in experiments performed at 37°C. This was not due to the low-temperature-associated increase in reservoir fluid resistance between the two current passing electrodes since we measured and corrected for fluid resistance in all experiments. Morphologically, these tissues still demonstrated reduced cytoplasmic density in ~10–40% of villus absorptive cells (Fig. 13) and collapse

FIGURE 6 Electron micrograph of mucosal sheet exposed to 600 mosM mucosal buffer. Areas with subjunctional evaginations (*E*) also frequently displayed perijunctional ballooning of the apical membrane with loss of surface microvilli (arrowheads) and associated thickening of the terminal web. (*TW*). × 19,500.

TABLE I

Comparison of Absorptive-Cell Tight-Junction Strand Counts and Depths in Control Sheets versus Those Exposed to 600 mosM Mucosal Buffer for 20 min

	Strand count	*n*	Tight-junction depth	*n*
			nm	
Control	5.3 ± 0.1	206	266 ± 6	210
600 mosM, mucosa	6.3 ± 0.2	167	303 ± 13	168
P	<0.005		<0.005	

Hyperosmotically exposed sheets show significant increases in mean depths and strand counts.

at the absorptive-cell-associated paracellular spaces. However, subjunctional evaginations of the lateral membrane with associated microfilament arrays were not found in these tissues. Examination of five freeze-fracture replicas of mucosal sheets exposed to 600 mosM M for 20 min at 4°C showed focal morphologic evidence of a phase transition on the lateral membrane (Fig. 14): Intramembrane particles were segregated into dense patches with intervening membrane faces devoid of particles. In addition, in no instance were foci of absorptive-cell tight junctions seen that were structurally similar to the deep, multistranded foci of tight junctions observed in mucosal sheets exposed to mucosal 600 mosM buffer at 37°C.

Effects of Osmotically Induced Resistance Rise on Dilution Potentials

Dilution of mucosal Na^+ and Cl^- by 10% with isotonic mannitol resulted in potential difference increments of +1.25 mV (mucosa positive) in control and +0.8 mV in 600 mosM pre-exposed mucosal sheets (NS). However, 20% mucosal dilution resulted in +2.5-mV increments in control but only +0.8-mV increments in 600 mosM pre-exposed sheets ($P < 0.001$; Fig. 15). At 4°C, 20% mucosal dilution potentials of isotonically bathed sheets were +0.9 mV ± 0.3 mV ($n = 4$) and 20% mucosal dilution potentials of 600 mosM pre-exposed sheets were +0.4 mV ± 0.3 mV.

DISCUSSION

We show that exposure for 20 min of the mucosa of guinea pig proximal jejunum to buffers made hyperosmotic by mannitol is accompanied by a substantial increase in transepithelial resistance. The magnitude of this resistance response is reduced by some agents that interfere with cytoskeletal function and is ablated at temperatures with induce, functionally (18) and morphologically, liquid-crystalline to gel phase transition of the lateral plasma membrane lipids and thus restrict the mobility of lateral membrane molecules. In concert with the hyperosmotically induced resistance rise, many villus

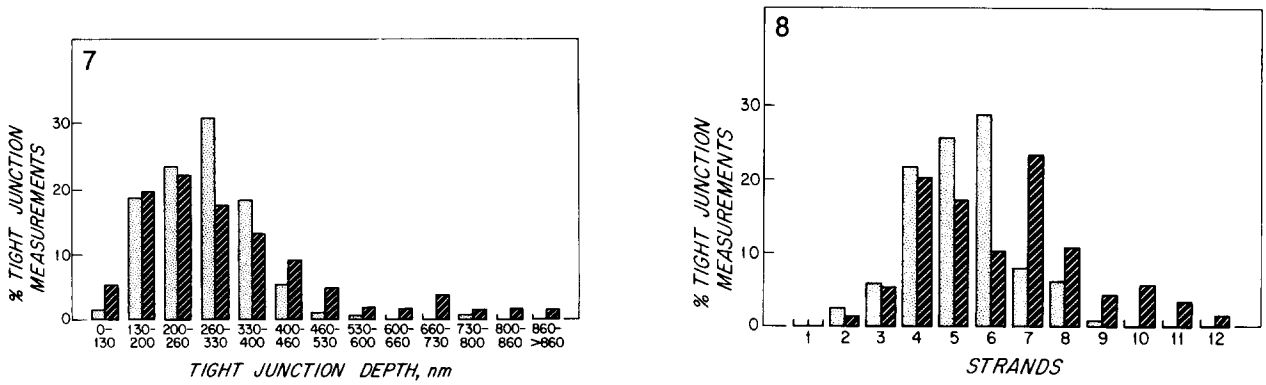

FIGURES 7 and 8 Histograms show frequency distribution of absorptive-cell depth measurements (Fig. 7) (left) and strand counts (Fig. 8) (right) in control (dotted bars) and 600 mosM mucosa (striped bars) exposed sheets. The increases in the mean values of these parameters of tight-junction structure after hyperosmotic mucosal exposure are not due to uniform shifts of tight-junction populations. Rather, new subpopulations of tight junctions characterized by multiple strands and extreme depths account for these changes.

absorptive cells undergo morphological alterations: Both the cytoplasmic electron density and affinity for toluidine blue decrease in a subpopulation of absorptive cells; subjunctional cytoplasmic protrusions associated with plaques of microfilaments form; apical membranes often lose parajunctional microvilli and become convex; and tight junctions show focal changes in structure characterized by greater depth and strand count. However, cells other than absorptive cells were structurally unaffected. As noted previously in rabbit gallbladder (1, 2), hyperosmotic mucosal exposure resulted in a collapse of intestinal epithelial paracellular spaces. However, we noted no apparent difference in the degree of collapse between those osmotically challenged tissues that were exposed to agents that inhibited the rise in resistance and those that were not. Mucosal osmotic loads not only increase jejunal transepithelial resistance and alter tight-junction structure but also cause a change in junctional charge selectivity, as assessed with dilution potentials.

Structural Site of Increased Transepithelial Resistance Induced by Mucosal Hyperosmotic Loads

Since, in buffer solutions, electrical current is carried by ions, transepithelial electrical resistance is viewed as resistance to the passive flow of ions. The two major pathways for such flow are (*a*) through the apical and basolateral membranes in series (transcellular) and (*b*) through the paracellular space. However, the resistance of biological membranes in series, although somewhat variable, is usually relatively high, often >1,000 $\Omega \cdot cm^2$ (19–22). Thus, in epithelia of relatively lower resistance, such as the small intestine, the vast majority of passive ion flow presumably occurs through the paracellular space. Indeed, in rabbit ileum 82% of passive transepithelial diffusion of sodium, potassium, and chloride occurs via the paracellular pathway (23). Thus, since paracellular flow may account for most of the passive ion flow in low-resistance epithelia and since transcellular resistance is very high, manipulations that result in increased transepithelial resistance are likely to do so by increasing the resistance of the paracellular pathway. The paracellular pathway may also be split into two components that may influence resistance: the tight junction and the remainder of the paracellular space. Since (*a*) the paracellular flow of tracer molecules is inhibited at the site of the tight junction (5–10), (*b*) tight junction structure generally correlates with transepithelial resistance (11, 12), and (*c*) experimental manipulations that alter tight junction structure often affect transepithelial resistance (9, 10), it is generally assumed that the tight junction and not the paracellular space is the barrier to paracellular flow of ions. However, based on data from studies of osmotic effects on another low-resistance epithelium, rabbit gallbladder, it has been suggested that paracellular pathway resistance may be increased under conditions in which the paracellular space is collapsed (1, 2, 24). Like jejunal epithelium, rabbit gallbladder, shows dose-dependent increases in transepithelial resistance in the 20-min period following mucosal, but not serosal, hypertonic loads (1). The dominant change described in electron micrographs of thin sections prepared from gallbladders exposed to mucosal osmotic loads was collapse of the lateral intercellular spaces. When mucosal bath osmolality was made hypertonic with sucrose, unidirectional sucrose flux increased in a nonlinear fashion with increasing mucosal sucrose concentrations. Indeed, when 300 mM sucrose was added to the mucosal buffer, sucrose permeability actually decreased by 75% (1). Likewise, increases in the tonicity of the mucosal, but not serosal, buffer decreased bidirectional permeability to 1,4 butanediol (1). Thus, these authors suggested that diffusion along the nonjunctional paracellular space was rate limiting under conditions of paracellular space collapse. In support of this contention, hydraulic conductivity was shown to be asymmetric in this epithelium with less osmotic water flow in the serosal-to-mucosal direction (mucosal hypertonic [1], increased resistance [24]) than in the mucosal-to-serosal direction (serosal hypertonic [1], normal resistance [24]). Such data would raise the possibility that the asymmetry of osmotic volume flow caused the discrepant transepithelial resistance readings in these two states if other parameters of the paracellular pathway, such as tight-junction structure and resistivity, were unchanged. If, however, tight-junction resistivity were increased with mucosal but not serosal osmotic loading, then the associated decrease in serosal-to-mucosal hydraulic conductivity might be more logically interpreted as secondary to altered junctional conductance. Such an explanation would also resolve the difficult problem of apparent asymmetry of hydraulic conductivity, which this tissue displays (1). While the increment of resistance change in response to mucosal osmotic loads reported by these authors was highly sensitive

FIGURE 9 Freeze-fracture replicas of absorptive-cell tight junctions (*A*) Tight junction from control mucosal sheets displaying uniform depth and composition. (*B* and *C*) Tight junctions from mucosal sheets exposed to 600 mosM mucosal buffer for 20 min. Focally, junctional depth and strand counts (arrowheads) are large. In addition, the perijunctional apical membranes (asterisk) associated with these junctional areas are bulging and relatively devoid of microvilli. Thus, these areas may correspond with electron microscopic images such as those in Fig. 5. × 70,000. A three-cell junction (*3CJ*) is present in the center of *B*, and increases in junction depth and strand count can be seen extending laterally from it in both directions. The arrow in the upper right hand corners of these and subsequent replicas indicate the direction of platinum shadowing.

to the size of the transepithelial osmotic gradient, gradients ranging from 50 to 300 mM produced similar degrees of paracellular space collapse (1). Furthermore, although these authors report no discernible difference in tight-junction structure as analyzed with thin sections, they do note that the plasma membranes of adjacent cells focally produced pentalaminar structures reminiscent of tight junctions in areas of cytoplasmic evaginations (1). Our study raises questions regarding the importance of paracellular space collapse as a major factor in the osmotically induced rise in transepithelial resistance, however. We were able to substantially inhibit the osmotically induced rise in transepithelial-resistance in jejunal epithelium with cytochalasin D but observed collapse of the paracellular space that was comparable with that observed in the absence of cytochalasin D. Determinations of paracellular space diameter derived from electron microscopic observations must be viewed with caution, however, for it is possible that commonly used fixation procedures may lead to altera-

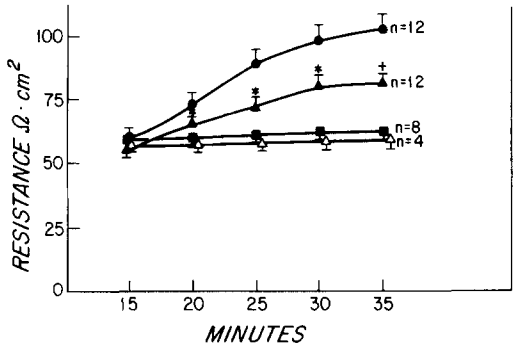

FIGURE 10 Effect of preincubation with 5 μg/ml cytochalasin D on mucosal 600 mosM-induced resistance increase. Cytochalasin D partially inhibits the increase in transepithelial resistance. * = $P <$ 0.02, + = $P < 0.01$. Comparisons are between 600 mosM exposed tissues with and without cytochalasin exposure. ●, 600 mosM mucosa, control; ■, normal Ringer's, control; Δ 5 μg/ml cytochalasin D, control; ▲ 5 μg/ml pretreated cytochalasin D, 600 mosM mucosa.

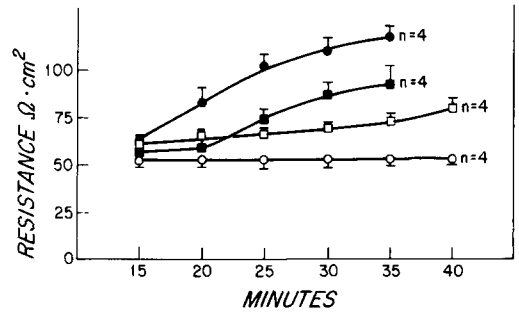

FIGURE 11 Effect of the plant cytokinin zeatin on the 600 mosM-induced increase in transepithelial resistance of mucosal sheets. Exposure of mucosal sheets to 1.25 mM zeatin produced resistance increments in the absence of osmotic gradients ($P < 0.05$ at 30 min and <0.01 at 40 min). However, this concentration of zeatin also inhibits ($P < 0.05$) the 600 mosM-induced rise in transepithelial resistance. O, isotonic control; ●, 600 mosM mucosa; □, 1.25 M zeatin control; ■, 1.25 M pretreated zeatin, 600 mosM mucosa.

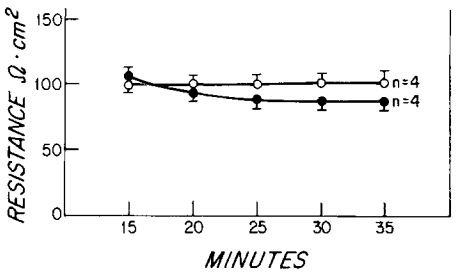

FIGURE 12 Low temperature (4°C) ablates the 600-mosM-induced rise in transepithelial resistance. O, isotonic control (4°C); ● 600 mosM mucosa (4°C).

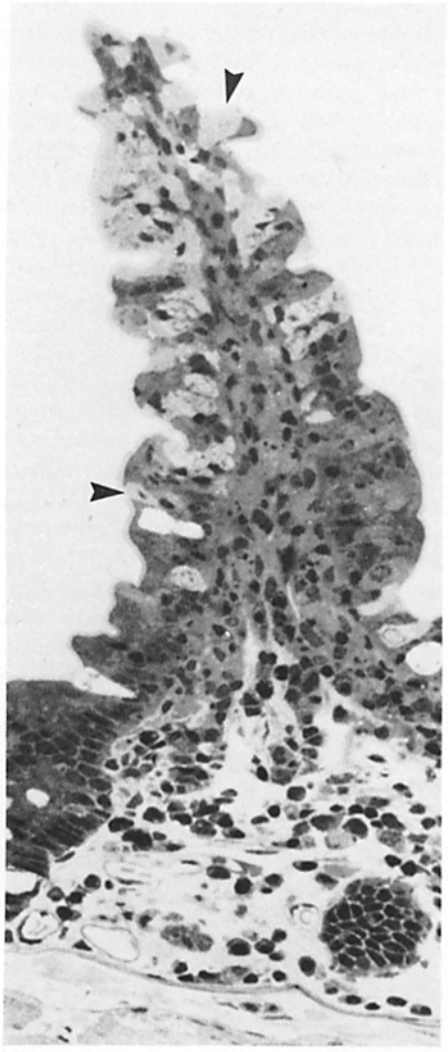

FIGURE 13 Light micrograph of mucosal sheet exposed to 600 mosM mucosal buffer for 20 min at 4°C. Although the transepithelial resistance did not rise in this sheet, it still shows many lucent absorptive cells (arrowheads) similar to those in sheets exposed at 37°C. × 250.

tions in the geometry of cells and the width of paracellular spaces (25–26). Still, postfixation observations probably reflect, to some degree at least, the natural geometry of paracellular spaces. For example, dilated intercellular spaces are observed if ileal loops are exposed to conditions that stimulate fluid transport before fixation (27). Similarly, observations of the size of the paracellular space in living *Necturus* gallbladder epithelium under various states of fluid transport correlate

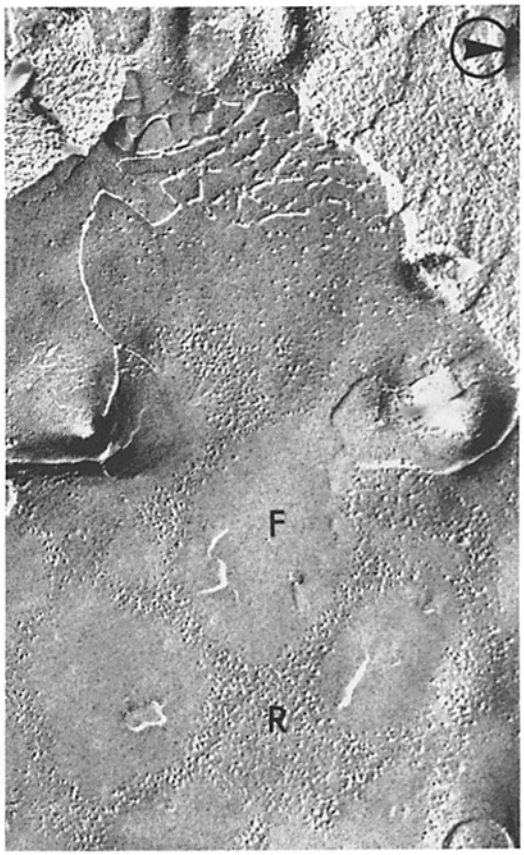

FIGURE 14 Freeze-fracture replica of absorptive-cell P-face lateral membrane exposed to 600 mosM mucosal buffer for 20 min at 4°C and subsequently fixed in the chamber. The lateral membrane displays formation of intramembrane-particle-free zones (*F*) which presumably represent crystallized membrane lipids surrounded by particle-rich (*R*) aisles. This appearance is consistent with fixation of tissue in a state of lateral membrane phase transition. × 74,000.

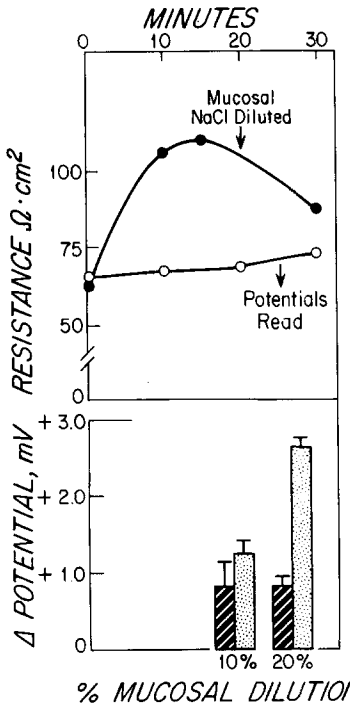

FIGURE 15 Effects of 600 mosM-induced high resistance state on mucosal NaCl dilution potentials. At the peak of the resistance response, the 600 mosM mucosal bath was reversed to isotonic buffer. When the potential difference had stabilized, mucosal NaCl was diluted by removing 10 or 20% of the mucosal buffer and replacing it with isotonic mannitol. The resulting potential difference was then read when it had again stabilized, and the result was expressed as increment from base-line potential. During the high resistance state, 20% dilution potentials were decreased from control values ($P < 0.01$). *Top*: ●, 600 mosM; O, control. *Bottom*: striped bars, 600 mosM; dotted bars, control.

well with observations derived from electron microscopic examination of this epithelium (28).

We show that alterations in the structure of jejunal absorptive-cell tight junctions may occur within minutes. However, this epithelium does not appear unique in this regard. Excised rat ventral prostate epithelium incubated at 37°C displays a sixfold expansion of net tight-junction strand length within 5 min (13). Furthermore, within 10 min of exposure of *Necturus* gallbladder epithelium to cAMP, transepithelial resistance begins to increase and peaks within 30–75 min at resistance levels ~60% greater than base line (14). Since *Necturus* gallbladder epithelium is of relatively low resistance (~100 $\Omega \cdot cm^2$), increments in resistance would most likely reflect increases in paracellular, not transcellular, resistance. Indeed, microelectrode studies show that apical membrane resistance dramatically decreased during this response (14). Moreover, no structural alterations in the intercellular space were noted, but quantitation of the freeze-fracture appearance of tight-junction structure showed significant increases in both tight-junction strand count and tight-junction depth (14).

Potential Cytoskeletal Influence of Tight-Junction Resistance

The mechanism(s) by which dispartate conditions such as elevations of intracellular cAMP in *Necturus* gallbladder and brief mucosal osmotic loads in guinea pig jejunum result in similar structural and functional modifications of tight junctions are unclear. However, we found focal subjunctional arrays of microfilaments in animals exposed to mucosal osmotic loads. Furthermore, we produced partial inhibition of the osmotically induced increase in transepithelial resistance by using cytochalasin D, which inhibits microfilament function. Subjunctional microfilament arrays were also noted to accompany the cAMP-induced rise in resistance in *Necturus* gallbladder (14) and, although these authors did not study the effects of agents that influence cytoskeletal function on the resistance response, a subunit of cAMP is known to interact with components of the cytoskeleton (29). It would not be surprising if tight-junction structure were influenced by the cytoskeleton since cytoskeletal elements appear to associate with the lateral membrane, particularly in the zone of the junctional complex of intestinal epithelial cells (30). In fact, alpha-actinin, a protein commonly found at sites of apparent attachment of microfilaments to plasma membranes (31–34), has been localized to the cytoplasmic region adjacent to the tight junction of intestinal epithelial cells (35). Moreover, agents that influence the cytoskeleton also affect paracellular resistance in other cell systems. For example, cytochalasin B has been shown to decrease the transepithelial resistance of confluent MDCK monolayers (36). Specifically, this change appears to be due to an alteration of paracellular pathway resistance, since scanning the monolayer surface with voltage-sensitive microelectrodes after exposure to cytochalasin B reveals a new population of low-resistance sites at zones of intercellular contact (36). Although agents that influence cytoskeletal function have been shown to produce alterations in either transepithelial resistance or tight-junction structure in a variety of epithelia (15, 36), the effect of these agents varies with dose, tissue, and the specific analogue used. For example, while exposure of *Necturus* gallbladder to 1.5 μm cytochalasin B produces increases in transepithelial resistance, higher doses decrease resistance (15). Transepithelial resistance of this epithelium also rises after exposure to the plant cytokinins zeatin and kinetin, and these changes are accompanied by alterations in tight-junction structure (15). In contrast with the above studies, we found no effect of either cytochalasin B and D or kinetin on base-line jejunal resistance even though the single doses we studied were the same doses that affected resistance in *Necturus* gallbladder. However, zeatin did produce resistance increments in jejunal epithelium. Furthermore, cytochalasin D and zeatin did inhibit the osmotically induced resistance increase but produced no obvious alterations in absorptive-cell cytoskeletal structure as assessed by electron microscopy. Agents that influence the cytoskeleton may affect the movement of cell surface molecules (37, 38) to which they are presumably attached (39); thus, these agents may exert effects on transepithelial resistance by influencing the movement of tight-junction subunits within the plasma membrane. Similarly, more extensive restriction of the mobility of tight-junction subunits could account for our finding that both the increase in osmotically induced resistance and the alteration in absorptive-cell tight-junction structure could be prevented when tissues were maintained at a temperature below that which induced phase transition of absorptive-cell basolateral membranes. Lastly, in view of the proposed logarithmic relationship between junctional resistance and strand count (40), it is not surprising that the modest increases in strand counts that we found were accompanied by striking increases in transepithelial resistance.

Although one striking morphological effect of mucosal 600 mosM loads was the production of absorptive cells with electron-lucent cytoplasm, such cells were also noted after 600 mosM exposure at 4°C. Furthermore, the perijunctional structural alterations noted by electron microscopy of thin sections occurred in both lucent and nonlucent cells. Thus, the relationship of this structural feature to the resistance response is unclear. Such cells might be produced by pertubation of the apical membrane with subsequent leak of lumenal solute into the cell cytoplasm. The resulting intracellular osmotic load could then induce water flow across the basolateral membrane into the cell, resulting in cytoplasmic clearing and cell swelling. Although we did not measure cell volumes, it did appear to us that lucent cells were swollen. Epithelial cell swelling has been reported in other systems under conditions of similar mucosal-to-serosal osmotic gradients (26).

Effect of Altered Tight-Junction Structure on Charge Selectivity

Our findings suggest that osmotic loads applied to jejunal mucosa not only alter absorptive-cell tight-junction structure but also alter tight-junction charge selectivity. Many, but not all (41), epithelial tight junctions, including those of mammalian small intestine (42) and gallbladder (43), and of amphibian urinary bladder (44) and skin (45), are cation selective. The degree of charge selectivity can be assessed in Ussing chambers by replacing a portion of Na^+ and Cl^- in the mucosal bath with equiosmolar portions of molecules with high reflection co-efficients. Mucosal-to-serosal gradients of Na^+ and Cl^- are thus produced in the absence of osmotic gradients. If these ions encounter a charge-selective tight junction while moving down this concentration gradient, a transjunctional electrical potential, termed a dilution potential, is produced and its size in millivolts reflects the magnitude

of the charge selectivity. If the increase in junctional depth and strand count that we detect after mucosal hyperosmotic exposure resulted from recruitment of additional normally functioning tight-junction subunits, one might expect cation selectivity to increase rather than decrease. The observed decrease indicates that either tight-junction cation selectivity has decreased or anion selectivity has increased. Since this alteration in charge selectivity is accompanied by an overall increase in tissue resistance, it cannot have been caused by an increase in anion selectivity alone. Thus the majority of the alteration in charge selectivity presumably resulted from a decrease in the cation permeability of the tight junction. Additionally, it is important to stress that this loss of charge selectivity cannot be attributed to nonspecific cell damage resulting in an increase in transcellular flux of all ion species regardless of charge. This interpretation would require that net transepithelial resistance to passive ion conductance be decreased, and we show that resistance is dramatically and significantly increased. The cAMP-induced rapid expansion of tight junctions seen in *Necturus* gallbladder is also accompanied by decreases in mucosal dilution potentials (14). Similar alterations in the charge selectivity of tight junctions might account for the fluctuations in transepithelial potential difference reported in rabbit gallbladder exposed to mucosal hyperosmotic loads by Wright et al. (24). Such exposure, which initiates flow of ions from serosal to mucosal baths, results in immediate increments in transepithelial potential difference which subsequently decline. Moreover, the decay in the potential temporally parallels the rise in transepithelial resistance, both having a half-life of ~10 min (24). Lastly, as the rate of the initial rise of transepithelial resistance is increased by increasing the osmotic gradient, the rate of potential difference decay is similarly accelerated (24). Although these data were interpreted as possibly reflecting a rapid, osmotically produced, fluctuation in the depth of serosal unstirred layers, these fluctuations might alternatively be interpreted as reflecting a rapid decrease in net tight-junction charge selectivity, an interpretation that would be consistent with our findings in jejunal epithelium and with those of Duffy et al. in cAMP-stimulated *Necturus* gallbladder (14). However, we also found that while 4°C ablated the 600 mosM resistance rise it did not totally prevent the decrease in the size of the 20% dilution potentials. Thus, the alteration of junctional charge selectivity does not appear to depend fully on the recruitment of new junctional subunits and may depend on other factors such as conformational changes within the tight-junction subunits. We also found that, at 4°C, dilution potentials were less than those at 37°C even in the absence of any osmotic gradient. Perhaps, subtle conformational changes in the tight junction resulting in altered charge selectivity might occur in the presence of gel phase lipids. That such conformational changes might occur in junctional subunits under conditions of membrane phase transition would not be surprising since both lateral and vertical displacement of integral membrane proteins occur during lipid phase transitions in other plasma membranes (46).

Conclusions and Their Potential Physiological Importance

We conclude that the progressive rise, over 20 min, in proximal jejunal transepithelial resistance induced by mucosal hyperosmotic loads may be attributable primarily to accompanying changes in tight-junction structure that result in increased transjunctional resistance. Furthermore, this modulation in tight-junction structure may be controlled by elements of the cytoskeleton and is accompanied by alterations in tight-junctional charge selectivity. Thus, alterations in the mucosal environment may potentially modulate the permeability characteristics of the paracellular shunt pathway. Such alterations in jejunal absorptive-cell tight-junction structure associated with transient mucosal osmotic loads may influence normal function of the small intestine. In humans given osmotically rich meals, hyperosmotic gastric contents are intermittently discharged into the proximal small intestine (47). We speculate that transient increases in transepithelial resistance in response to these brief hyperosmotic loads could serve as a protective mechanism that regulates the rate of fluid flux from the lamina propria into the lumen. Secondly, decreases in net tight-junction charge selectivity would permit transepithelial transfer of water from the lamina propria to the lumen without necessitating development of large transepithelial charge gradients that might otherwise occur as a consequence of solvent drag. Lastly, if alterations in net charge selectivity reflect a decrease in cation permeability, such alterations could aid in protecting the lamina propria from back fluxes of the H^+ which accompanies osmotic loads of gastric origin.

I am grateful to Dr. J. S. Trier for his continued encouragement and to Dr. Trier, Dr. M. Field, and Dr. H. Rennke for critically reviewing the manuscript. I thank Dr. M. Karnovsky for reviewing with me much of the data presented here; Ms. Susan Carlson for her expert technical assistance; and Ms. Valerie Sherman for preparing the manuscript.

This work was supported by research grant AM 27972 from the National Institutes of Health.

Received for publication 27 September 1982, and in revised form 24 March 1983.

REFERENCES

1. Smulders, A. P., J. M. Tormey, and E. M. Wright. 1972. Effect of osmotically induced water flows on the permeability and ultrastructure of the rabbit gallbladder. *J. Membr. Biol.* 7:164–197.
2. Bindslev, N., J. M. Tormey, and E. M. Wright. 1974. The effects of electrical and osmotic gradients on lateral intercellular spaces and membrane conductance in a low resistance epithelium. *J. Membr. Biol.* 19:357–380.
3. Powell, D. W. Barrier function of epithelia. 1981. *Am. J. Physiol.* 241:6275–6288.
4. Wiedner, G., E. M. Wright. 1975. The role of the lateral intercellular spaces in the control of ion permeation across the rabbit gallbladder. *Pfluegers Arch.* 358:27–40.
5. Erlij, D., and A. M. Martinez-Palomo. 1972. Opening of tight junctions in frog skin by hypertonic urea solutions. *J. Membr. Biol.* 9:229–240.
6. Cereijido, M., E. Stefani, and A. M. Martinez-Palomo. 1980. Occluding junctions in a cultured transporting epithelium: structural and functional heterogeneity. *J. Membr. Biol.* 53:19–32.
7. Madara, J. L., and J. S. Trier. 1982. Structure and permeability of Goblet cell tight junctions in rat small intestine. *J. Membr. Biol.* 66:1–13.
8. Civan, M. M., and D. R. DiBona. 1978. Pathways for movement of ions and water across toad urinary bladder. III. Physiological significance of the paracellular pathway. *J. Membr. Biol.* 38:359–386.
9. Wade, J. B., J. P. Revel, and V. A. DiScala. 1973. Effect of osmotic gradients on intercellular junctions of the toad bladder. *Am. J. Physiol.* 224:407–415.
10. Wade, J. B., and M. J. Karnovsky. 1974. Fracture faces of osmotically disrupted zonulae occludentes. *J. Cell Biol.* 62:334–350.
11. Claude, P., and D. A. Goodenough. 1973. Fracture faces of zonulae occludentes from "tight" and leaky" epithelia. *J. Cell Biol.* 58:390–400.
12. Pricam, C., F. Humbert, A. Perrelet, and L. Orci. 1974. A freeze-etch study of the tight junctions of the rat kidney tubules. *Lab. Invest.* 30:286–291.
13. Kachar, B., and P. Pinto da Silva. 1981. Rapid massive assembly of tight junction strands. *Science (Wash. DC).* 213:541–544.
14. Duffey, M. E., B. Hainau, S. Ho, and C. J. Bentzel. 1981. Regulation of epithelial tight junction permeability by cyclic AMP. *Nature (Lond.).* 204:451–453.
15. Bentzel, C. J., B. Hainau, S. Ho, S. W. Hui, A. Edelman, T. Anagnostopoulos, and E. L. Beneditti. 1980. Cytoplasmic regulation of tight-junction permeability: effect of plant cytokinins. *Am. J. Physiol.* 239:C75–C89.
16. Karnovsky, M. J. 1965. A formaldehyde-glutaraldehyde fixative of high osmolality for use in electron microscopy. *J. Cell Biol.* 27(2, Pt. 2):137*a*. (Abstr.)
17. Kagnoff, M. F., R. M. Donaldson, and J. S. Trier. 1972. Organ culture of rabbit small

intestine: prolonged in vitro steady state protein synthesis and secretion and secretory IgA secretion. *Gastroenterology.* 63:541–551.
18. Brasitus, T. A., A. R. Tall, and D. Schachter. 1980. Thermotropic transitions in rat intestinal plasma membranes studied by differential scanning calorimetry and fluorescence polarization. *Biochemistry.* 19:1256–1261.
19. Henin, S. D., Cremaschi, T. Schettino, G. Meyer, C. L. L. Donin, and F. Cotelli. 1977. Electrical parameters in gallbladders of different species: their contribution to the origin of the transmural potential difference. *J. Membr. Biol.* 34:73–91.
20. Schultz, S. G., R. A. Frizzell, and H. N. Nellans. 1977. Active sodium transport and the electrophysiology of rabbit colon. *J. Membr. Biol.* 33:351–384.
21. Spenney, J. G., R. L. Shoemaker, and G. Sachs. 1974. Microelectrode studies of fundic gastric mucosa: cellular coupling and shunt conductance. 19:105–128.
22. Reuss, L., and A. L. Finn. 1974. Passive electrical properties of toad urinary bladder epithelium: intercellular electrical coupling and transepithelial cellular shunt conductances. *J. Gen. Physiol.* 64:1–25.
23. Frizzell, R. A., S. G. Schultz. 1972. Ionic conductances of extracellular shunt pathway in rabbit ileum. Influence of shunt on transmural sodium transport and electrical potential differences. *J. Gen. Physiol.* 59:319–346.
24. Wright, E. M., A. P. Smulders, and J. M. Tormey. 1972. The role of the lateral intercellular spaces and solute polarization effects in the passive flow of water across the rabbit gallbladder. *J. Membr. Biol.* 7:198–219.
25. Fredericksen, J., and J. Rostgaard. 1974. Absence of dilated lateral intercellular spaces in fluid transporting frog gallbladder epithelium. Direct Microscopy Observations. *J. Cell Biol.* 61:830–834.
26. Bentzel, C. J., G. Parsa, and D. K. Hare. 1969. Osmotic flow across proximal tubule of *Necturus*: Correlation of physiologic and anatomic studies. *Am. J. Physiol.* 217:570–580.
27. Tomasini, J. T., and W. O. Dobbins. 1970. Intestinal mucosal morphology during water and electrolyte absorptive. A light and electron microscopic study. *Dig. Dis. Sci.* 15:226–238.
28. Spring, K. R., and A. Hope. 1978. Size and shape of the lateral intercellular spaces in a living epithelium. *Science (Wash. DC).* 200:54–57.
29. Rasenick, M. M., P. J. Stein, and M. W. Bitensky. 1981. The regulatory subunit of adenylate cyclase interacts with cytoskeletal components. *Nature (Lond.).* 294:560–562.
30. Bretscher, A., and K. Weber. 1978. Localization of actin and microfilament-associated proteins in the microvilli and terminal web of the intestinal brush border by immunofluorescence microscopy. *J. Cell Biol.* 79:839–845.
31. Puszin, S., E. Puszin, J. Maimon, C. Rauault, W. Schook, C. Ores, S. Kochwa, and R. Rosenfield. 1978. Alpha-actinin and trophomyosin interactions with a hybrid complex of erythrocyte actin and muscle-myosin. *J. Biol. Chem.* 252:5529–5537.
32. Schollmeyer, J. E., L. T. Furcht, R. E. Goll, R. M. Robson, and M. M. Stroner. 1976. Localization of contractile proteins in smooth muscle cells and in normal and transformed fibroblasts. *Cold Spring Harbor Conf. Cell Prolif.* 3(Book A):361–388.
33. Lazanides, E., and K. Burridge. 1975. Alpha-actinin immunofluorescent localization of a muscle structural protein in nonmuscle cells. *Cell.* 6:289–298.
34. Fujiwara, K., M. E. Porter, and T. D. Pollard. 1977. Comparative localization of myosin, alpha-actinin, and tropomyosin in cultured cells by double fluorescent antibody staining. *J. Cell Biol.* 75(2, Pt. 2):267*a*. (Abstr.)
35. Craig, S. W., and Pardo, J. V. 1979. Alpha-actinin localization in the junctional complex of intestinal epithelial cells. *J. Cell Biol.* 80:203–210.
36. Meza, I., M. Sabanero, E. Stafani, and M. Cereijido. 1982. Occluding junctions in MDCK cells: modulation of transepithelial permeability by the cytoskeleton. *J. Cell. Biochem.* 18:407–421.
37. Yahara, I., and F. Kakimoto-Sameshima. 1978. Microtubule organization of lymphocytes and its modulation by patch and cap formation. *Cell.* 15:251–259.
38. Poste, G., D. Papahadjopoulos, and G. L. Nicholson. 1975. Local anesthetics affect transmembrane cytoskeletal control of mobility and distribution of cell surface receptors. *Proc. Natl. Acad. Sci. USA.* 72:4430–4434.
39. Gabbiani, G., C. Chaponnier, A. Zumbe, and P. Vassalli. 1977. Actin and tubulin co-cap with surface immunoglobulins in mouse B lymphocytes. *Nature (Lond.).* 269:697–698.
40. Claude, P. 1978. Morphological factors influencing transepithelial permeability: a model for the resistance of the zonula occludentes. *J. Membr. Biol.* 39:219–232.
41. Kauffman, G. L., and M. R. Thompson. 1975. Titration of sodium channels in canine gastric micosa. *Proc. Natl. Acad. Sci. USA.* 72:3731–3734.
42. Smyth, D. H., and E. M. Wright. 1966. Streaming potentials in the rat small intestine. *J. Physiol. (Lond.).* 182:591–602.
43. Wright, E. M., and J. M. Diamond. 1968. Effects of pH and polyvalent cations on the selective permeability of gallbladder epithelium to monovalent ions. *Biochem. Biophys. Acta.* 163:57–74.
44. Lipman, K. M., R. Dodelson, and R. M. Hays. 1966. The surface charge of isolated toad bladder epithelial cells: mobility, effect of pH and divalent ions. *J. Gen. Physiol.* 49:501–516.
45. Amberson, W. R., and H. Klein. 1978. The influence of pH upon the concentration potentials across the skin of the frog. *J. Gen. Physiol.* 11:823–840.
46. Armond, P. A., and L. A. Staehlin. 1979. Lateral and vertical displacement of integral membrane proteins during lipid phase transition in *Anacystic nidulans. Proc. Natl. Acad. Sci. USA.* 76:1901–1905.
47. Hunt, J. M. 1956. Some properties of an alimentary osmoreceptor mechanism. *J. Physiol. (Lond.).* 132:267–288.